Hydroclimatic modelling of local sea level rise and its projection in future

A. Naren & Rajib Maity

Theoretical and Applied Climatology

ISSN 0177-798X

Theor Appl Climatol
DOI 10.1007/s00704-016-1897-4

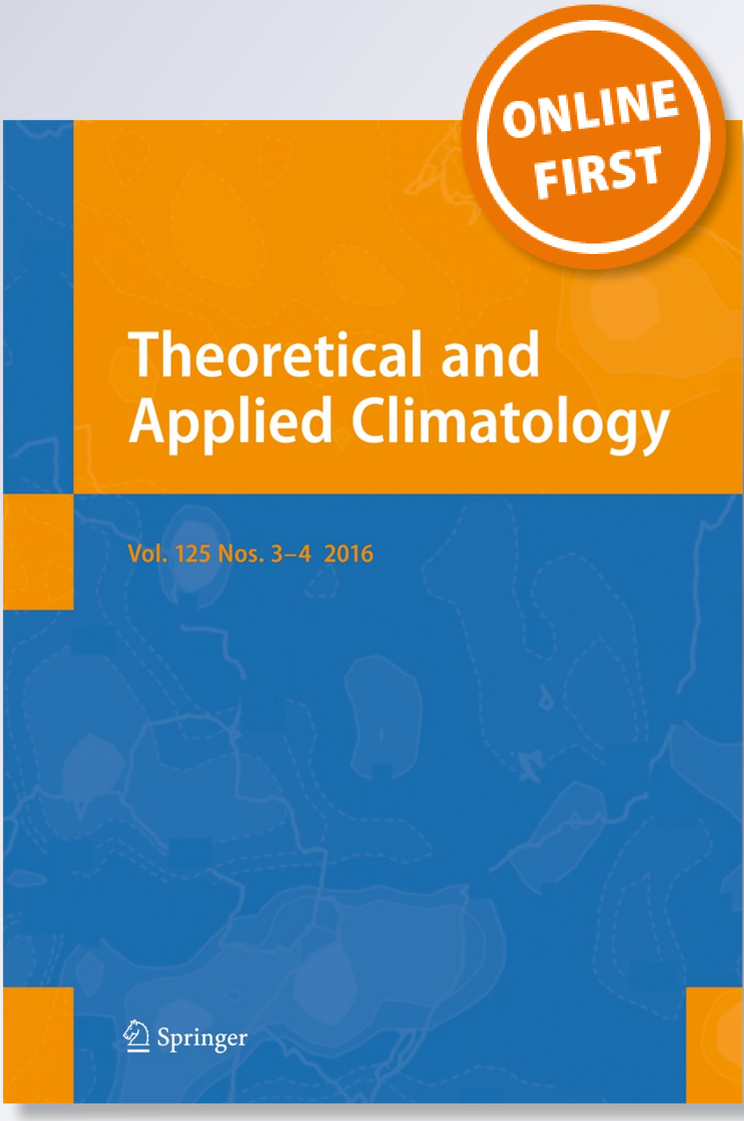

Theor Appl Climatol
DOI 10.1007/s00704-016-1897-4

ORIGINAL PAPER

Hydroclimatic modelling of local sea level rise and its projection in future

A. Naren [1] · Rajib Maity [1,2]

Received: 30 October 2015 / Accepted: 12 August 2016

Abstract Studies on sea level rise (SLR) in the context of climate change are gaining importance in the recent past. Whereas there is some clear evidence of SLR at global scale, its trend varies significantly from location to location. The role of different meteorological variables on sea level change (SLC) is explored. We hypothesise that the role of such variables varies from location to location and modelling of local SLC requires a proper identification of specific role of individual factors. After identifying a group of various local meteorological variables, Supervised Principal Component Analysis (SPCA) is used to develop a location specific Combined Index (CI). The SPCA ensures that the developed CI possesses highest possible association with the historical SLC at that location. Further, using the developed CI, an attempt is made to model the local sea level (LSL) variation in synchronous with the changing climate. The developed approach, termed as hydroclimatic semi-empirical approach, is found to be potential for local SLC at different coastal locations. The validated hydroclimatic approach is used for future projection of SLC at those coastal locations till 2100 for different climate change scenarios, i.e. different Representative Concentration Pathways (RCPs). Future hydrometeorological variables are obtained from Global Climate Models (GCMs) for different such scenarios, i.e. RCP2.6, RCP4.5 and RCP8.5. Effect of glacial isostatic readjustment (GIA) is not included in this study. However, if the reliable information on GIA is available for a location, the same can be arithmetically added to the final outcome of the proposed hydrometeorological approach.

✉ Rajib Maity
rajib@civil.iitkgp.ernet.in; rajibmaity@gmail.com

A. Naren
narenavailable@gmail.com

[1] Department of Civil Engineering, Indian Institute of Technology Kharagpur, Kharagpur, West Bengal 721302, India

[2] Karlsruhe Institute of Technology (KIT), Campus Alpin - IMK-IFU, Garmisch-Partenkirchen, Germany

1 Introduction

In the context of climate change, one of its important impacts on the coastal environment is the increase in sea level, threatening the coastal community and causing the region to submerge if the rise becomes pronounced. The mechanisms causing the sea level rise (SLR) and their interactions are complex in nature and hence difficult to understand. The process underlying any change in sea level (also called as sea level change, SLC) is a change in the combination of several atmospheric and oceanographic phenomena (Han and Huang 2009; Dogan et al. 2015). These climate sensitive processes over the period of years imply the SLC response as a cause of climate change which is widely distributed spatially and temporally throughout the world. The dynamics between climate change and SLC at a local scale is a complex process, making the prediction of SLR difficult. Complexity increases at local scale owing to its spatio-temporal distribution. This is the focus of this study—whether it is possible to extract the concurrent information of climatic variables that may have influence on the SLR at a local scale and exploiting this information how effectively the local SLR can be simulated?

Earlier studies were attempted to simulate the global mean sea level (GMSL) following the emission scenarios reported by IPCC with some underlying uncertainties (Rahmstorf, 2007; Meehl et al. 2007a, b; Vermeer and Rahmstorf, 2009; Jevrejeva et al. 2009; Solomon et al. 2009; Grinsted et al. 2010; Jevrejeva et al., 2010; Kemp et al. 2011; Pardaens

Published online: 01 September 2016

et al., 2011). In general, earlier studies on predicting GMSL were carried out under the basic assumption that SLC varies linearly with the climate forcing. The majority of such studies took the global temperature as the only predictor of the climate forcing responsible for SLC. The emission scenarios adopted by the IPCC fifth assessment report (AR5) for greenhouse gas concentration are called as Representative Concentration Pathways (RCPs). The AR5 projection of global average of SLR is in the range of 0.26 m for RCP2.6 scenario to 0.98 m for RCP8.5 scenario by 2100. However, local SLR significantly deviates from the global (Church and Clark, 2013). The cause for such deviation and its relevance were studied by Milne et al. (2009) and Stammer et al. (2013). There are variety of factors such as the expansion of warming water, salinity and ice sheet melting (Levermann et al., 2013; Yin et al. 2009), changes in the static equilibrium sea level configuration, produced by the gravitational, elastic and rotational effects of mass redistribution (Kopp et al. 2010) coupled atmospheric oceanic climate patterns such as El-Niño Southern Oscillation (ENSO) and others (Bindoff et al. 2007).

Earlier studies on the modelling of local SLR were carried out for Netherlands (Katsman et al. 2011), New York City (Horton et al. 2011; NYCPCC 2013) and New Jersey (Miller et al. 2013). Kopp et al. (2014) projected the probabilistic set of sea level values for twenty-first and twenty-second century for a network of tide gauges distributed across the globe. Several studies have projected the local sea level across the globe using Coupled Model Intercomparsion Project version 5 (CMIP5) (Slangen et al. 2012; Perrette et al. 2013; Slangen et al. 2014). However, the GCM simulations suffer from a significant uncertainty and location-specific dynamics of SLR heavily depend on the concurrent influence of several hydroclimatic variables. The characteristics of different hydroclimatic variables with respect to their relationship with SLR are provided in Table 1 with relevant references. Objective of this paper is to explore the hydroclimatic variables causing the local SLR and to develop a location-specific, semi-empirical hydrometeorological model for SLR at local scale. The developed model is further utilized for future projections of local SLR upto the year 2100 for the RCP2.6, RCP4.5 and RCP8.5.

To achieve the proposed objective, first, a Combined Index (CI) that represents all the possibly influencing hydroclimatic variables is developed in such a way that it contains maximum possible information from each hydroclimatic variable. Next, the first-order time derivative of the local SLC is hypothesised to vary linearly with the CI. Earlier, a similar approach was followed by Rahmstorf (2007) for GMSL with respect to temperature only. It is true that each variable may have different extent of influence from one location to another. This should reflect in the coefficients of CI while combining the hydroclimatic inputs. Complete methodology is explained in the following section.

2 Proposed methodology

Using the hydroclimatic variables namely air temperature (ATP), zonal wind (UWN), meridional wind (VWN), sea level pressure (SLP) and precipitation (PPT) (henceforth called as 'set of input variables'), the local SLC is modelled in respect to the location-specific, combined influence of each of these variables. Though salinity may also be an important component for the local change in sea level, it is not included in our study because of the non-availability of the salinity data in many coastal parts across the world. By considering the set of input variables, the CI is developed. The idea of developing the CI is to reduce the dimensionality of the set of input variable and to assign the appropriate weightage to the individual input variables in order to ensure the maximum association with the target variable, i.e. SLC. Dimensionality reduction is generally carried out through principal component analysis (PCA) and considering first few principal components (PCs) that carry most of the variability in the set of input variables. However, in order to assign the location-specific relative weightages to the individual input variables, the procedure of dimensionality reduction should be supervised by the observed SLC at that location. Thus, for determining the CI and to examine the weightages of individual hydroclimatic variables, supervised principal component analysis (SPCA) proposed by Barshan et al. (2011) is adopted in this study. The detailed description of SPCA is provided in the following subsection.

2.1 Development of combined index using SPCA

The classical PCA is used for finding the uncorrelated orthogonal components of a high dimensional dataset in order of their variance explained, with first component storing the maximum variance. However, these components (coefficients having high variance) of the dataset do not consider the target variable. In other words, the PCA-generated components are independent of target variable, if any. Thus, such components may or may not have any correlation with the target variable to be modelled. On the other hand, the SPCA approach is a more general statistical framework, and PCA is a special form of the SPCA. The SPCA is 'supervised' by the target variable, and it is an efficient mathematical approach for finding out the orthogonal components of the input variables in such a way that the first component possesses the highest association with the target variable, i.e. SLC in our case. The square of the coefficients of this component also portrays the relative importance of the input variables to the SLC.

The procedure of SPCA as proposed in Barshan et al. (2011) is adopted in our study. Let $\mathbf{X}(\in R^p)$ is a p-dimensional vector of input variables, (i.e. 'set of input variables' as mentioned before) and $\mathbf{Y}$ is a 1-dimensional vector of the target variable, i.e. SLC. Assuming independent and identically

Table 1 Characteristics of hydroclimatic variables with respect to sea level rise

Hydroclimatic variable	Characteristics	Literatures
Air temperature	(i) The SLC caused by changes in air temperature alone constitutes the thermal expansion forcing part. (ii) Ocean warming dominates in absorbing the total thermal energy stored in the climate system. This causes the ocean temperature to increase resulting in decrease of the density and thereby ocean volume increases (steric sea level rise). (iii) The trend of globally averaged combined land and ocean surface temperature data shows a warming of 0.85 °C (0.65 to 1.06 °C) over the period 1880 to 2012. (iv) The relationship between the GMSL and air temperature is well established. (v) Water mass properties such as temperature and salinity are important for replicating LSL change.	Rahmstorf (2007), Vermeer and Rahmstorf (2009), Grinsted et al. (2010), Kemp et al. (2011), Suzuki and Ishii (2011)
Wind effects	(i) The wind is the driving force for transporting the warm ocean waters from one place to another. (ii) The drag of the wind on the ocean surface transfers energy and momentum to the relatively slow moving ocean surface layer. (iii) The zonal and meridional wind anomalies cause considerable changes in the LSL. (iv) Changes in upper ocean heat content in the tropical oceans strongly contribute to the regional characteristics of sea level anomalies on interannual to centennial scales.	Frankignoul et al. (1997), Hong et al. (2000), Lowe and Gregory (2006), Kolker and Hameed (2007), Timmermann et al. (2010)
Sea level pressure	(i) The sea level pressure changes are considered to affect the sea level like a reverse barometer that is an increase in sea level pressure will decrease the sea level and vice versa. (ii) An increase in sea level pressure of 1 mb will cause a variation of 1 cm of sea level approximately. (iii) The reverse barometric effect has been proved for its linkage to SLC (iv) The effect of sea level pressure is much pronounced in causing the sea level variations in the Baltic Sea. (v) Sea level pressure is able to explain much of the variance of the sea level of German Bight.	Wunsch and Stammer (1997), Hunicke and Zorita (2006), Albrecht and Weisse (2012)
Precipitation	(i) Changing climate phenomena may cause change in pattern of hydrological cycles, affecting the rainfall distribution, increasing/decreasing fresh water inflows from rivers into the sea and thereby affecting the spatial distribution of salinity and density that may have causative effects on the LSL change.	Bindoff et al. (2007)

distributed (i.i.d) samples, i.e. $\left[\left(x_1^p, y_1\right), \left(x_2^p, y_2\right), \cdots \left(x_n^p, y_n\right)\right]$, SPCA finds out an orthogonal matrix projection matrix (**U**) of size px1, such that **Y** is directly scaled on to the projected input matrix, $\mathbf{U}^{\mathrm{T}}\mathbf{X}$. The maximum dependency between $\mathbf{U}^{\mathrm{T}}\mathbf{X}$ and **Y** is found by using Hilbert Schmidt Independence Criterion (HSIC), necessitating the trace of matrix **KHLH**, to maximize, where **K** is the kernel of $\mathbf{U}^{\mathrm{T}}\mathbf{X}$ (e.g. $\mathbf{X}^{\mathrm{T}}\mathbf{U}\mathbf{U}^{\mathrm{T}}\mathbf{X}$) and **L** is the kernel of **Y** (e.g. $\mathbf{Y}^{\mathrm{T}}\mathbf{Y}$). Thus, the optimization problem of SPCA algorithm can be written as

$$\underset{u}{\operatorname{argmax}}\ \mathbf{tr}\left(\mathbf{U}^T \mathrm{XHLH}\mathbf{X}^T\mathbf{U}\right) = 1 \tag{1}$$

The solution of the optimization problem is the orthogonal transformation matrix **U**. This matrix is having the coefficients for different input variables, known as the SPCA coefficients. Square of these coefficients represents the percentage contribution (statistically) of each of the hydroclimatic input variable to cause the SLC.

In our study, the anomaly values of hydroclimatic inputs and the observed sea level data are used in the SPCA algorithm to keep aside the seasonal component, if any, while developing coefficient of the CI. The monthly anomaly values (deseasonalized data) of the hydroclimatic variables and the observed sea level are computed by subtracting the long term monthly means and dividing by its corresponding standard deviation. The general expression to compute the monthly anomaly values is

$$A_{ij} = \frac{A_{ij}^{org} - \mu_i}{\sigma_i} \tag{2}$$

where A_{ij} is the anomaly for ith month and jth year of study, A_{ij}^{org} is the actual value of the data for the ith month and jth year, μ_i is the long term mean of ith month and σ_i is the long term monthly standard deviation of ith month. Henceforth, A_{ij} is denoted as S_{ij} in case of sea level anomaly and as X_{ij}^* in case of a hydroclimatic input (indicated in the superscript *). The matrix notation of the set of all hydroclimatic inputs is denoted as the $\boldsymbol{X}_{ij}$.

Finally, the Combined Index (CI) is estimated by multiplying the coefficients of the orthogonal transformation matrix **U** with the set of hydroclimatic inputs as

$$CI_{ij} = \mathbf{U}^T \mathbf{X}_{ij} \tag{3}$$

where the subscript 'ij' indicates the time step as explained before.

2.2 Semi-empirical model for SLC using CI

The proposed semi-empirical model linking the rate of local SLC and hydroclimatic variables is expressed as

$$\frac{dS_{ij}}{dt} = \theta\, CI_{ij} + c \qquad for\ all\ \ i, j \tag{4}$$

where $\frac{dS}{dt}$ is the time rate of SLC anomaly, θ is the slope between the CI and $\frac{dS}{dt}$, c is the intercept value and CI is the 'Combined Index' that represents the combined information of all the hydroclimatic inputs. The magnitude of $\frac{dS}{dt}$ is assessed by the trend of the SLC over the recent past. In this analysis, 5-year moving average values of SLC is used to consider the overall trend and to avoid the shorter-term seasonal fluctuations at monthly scale.

The equation (4) is equivalent to fitting a linear relationship between the CI and first order time derivative of local SLC. In other words, linear trend component of the association between the rate of SLC and CI is modelled. The efficacy of this modelling philosophy is tested later while developing the model at different locations and assessing their performance. The model parameters (θ and c) are estimated during model development period and validated during the testing period.

The estimated values of SL anomaly, denoted as S_{ij}, are back transformed to original scale by

$$\hat{H}_{ij} = \left(\hat{S}_{ij}\sigma_i + \mu_i \right) \tag{5}$$

The model performance is assessed through (i) correlation coefficient (CC), (ii) root mean square error (RMSE) and (iii) degree of agreement (DoA) (Wilmot et al. 2012) during both model development and testing period. These statistics are computed between estimated sea level and observed sea level at different tide gauges.

Using the developed model, future projections of sea level upto the year 2100 is computed. For the projection purpose, GCM simulated hydroclimatic inputs are used from the Second Generation Earth System Model of the Canadian Centre for Climate Modelling and Analysis (CanESM2) for the IPCC future warming scenarios RCP2.6, RCP4.5 and RCP8.5. The time range of these projections is from the year 2006 to 2100. First, the sea level anomaly over the projection period is estimated through the proposed semi-empirical model. Since there is no projected LSL data available, the estimation of LSL is obtained by

$$\hat{H}_{ij} = \left(\hat{S}_{ij}\sigma_i + \mu_i \right) + GMSL_{ij} \tag{6}$$

where S_{ij} is the computed sea level anomaly in the projection period by using the proposed semi-empirical model, μ_i and σ_i are long term mean and standard deviation of the ith month computed from the historical record (model development period), and $GMSL_{ij}$ is the global average projection of mean sea level. If the GMSL is not added (Eq. 6), the projected values of local SLC would be valid with the assumption that GMSL will remain unchanged in future, which is not the case. Thus, the projected GMSL is added to the modelled LSL change to assess the overall effect of local SLC in the future (projection period, i.e. 2006–2100). It is obvious that the projected GMSL changes (or specifically speaking rises) over time but does not vary from one location to another location. It is also important to state that the error in the estimation of GMSL is not within the scope of this study. The values of global average projections can be obtained from any GCM output and discussed in the data used section.

2.3 Data collection

The monthly data for the four hydroclimatic input variables (ATP, SLP, UWN and VWN) are collected from the National Oceanic and Atmospheric Administration (NOAA) National Centre for Environmental Prediction/National Centre for Atmospheric Research (NCEP/NCAR) dataset. The NCEP/NCAR dataset is available from the year 1948 and has been constantly updated till date. The NCEP/NCAR catalogue does not have precipitation data for the entire analysis period starting from 1948. Hence, the observed monthly precipitation data is collected from the archives of the India Meteorological Department (IMD).

The monthly sea level data is obtained from the Permanent Service for Mean Sea Level (PSMSL). The data from PSMSL is supplied in two formats 'metric' and 'revised local reference' (RLR). The RLR dataset is taken 7 m below the MSL in order to avoid any negative values in the tide gauge record. This data is used widely for the sea level related analysis and IPCC projections. Aforementioned data on hydroclimatic input variables and sea level are used for model development and testing.

For future projection, the estimated GMSL and projected data of all the hydroclimatic input variables for the three future climate scenarios (RCP2.6, RCP4.5 and RCP8.5) from January 2006 to December 2100 are obtained from CanESM2. These data sets are available from http://www.ipcc-data.org/sim/gcm_monthly/AR5/Reference-Archive.html.

2.4 Details of the tide gauges

There are as many as 26 tide gauges of the PSMSL in India along the Bay of Bengal and Arabian Sea, having different length of available data. However, most of the tide gauges have incomplete dataset or have lot of missing data. Thus, out of 26, four tide gauges, having reasonably long records (more than 40 years) and less missing data, are considered. These four tide gauges are (i) Diamond Harbour, (ii) Kolkata (Garden Reach), (iii) Cochin and (iv) Mumbai (Apollo Bandar) (Fig. 1). The geographic coordinates and other details of the four tide gauges are given in Table 2.

2.5 Time period of analysis

The period of analysis is divided into three periods—(i) model development period, (ii) model testing period and (iii) model projection period. In this study, the missing data from the monthly record of PSMSL archives are treated as follows. If there is only a few monthly missing data scattered over the length of available records, it is filled up by taking the averages of at least 120 previous time steps monthly data. If there is missing data over a long, continuous period, say 6 months or longer, it is left out from the analysis. Next, the model development and model testing period for a particular monitoring station is decided based on the availability of monthly observed sea level data. The details of the model development, testing and projection periods for different tide gauges are shown in Table 3.

3 Results and discussion

The trend of the LSL at the particular location is assessed based on the 5-year moving averages of monthly SLC anomaly, as mentioned before. The plots of μ_i and σ_i for different tide gauges are shown in Fig. 2. The plots of the variation of observed sea level and observed sea level anomaly over the development period for different tide gauges are shown in Figs. 3 and 4, respectively. From Fig. 2, it can be observed that long term monthly standard deviation of sea level data at Kolkata tide gauge is maximum when compared to the other stations considered. Both the tide gauges Kolkata and Diamond Harbour are located on the banks of river Hoogly. Kolkata is almost 100 km inland from the sea coast, whereas Diamond Harbour is very near to the sea coast. It can be seen from Fig. 2 that the tendency of standard deviation of sea level at Kolkata is very different from Diamond Harbour, although both the tide gauges are located nearer. Kolkata tide gauge being located on Hoogly river is subjected to the river flow seasonality and sediment deposition taking place in the river beds. Both river flow seasonality and sedimentation can affect the sea level readings at Kolkata tide gauge. Hence, in order to account for possible deviation of readings, PSMSL carried out several corrections in the sea level record of Kolkata tide gauge in the past two decades. In this study, the latest updated observed sea level data (from PSMSL, updated on January 22, 2016) of Kolkata tide gauge is used. As mentioned before, the variation of Kolkata gauging site is more as compared to other

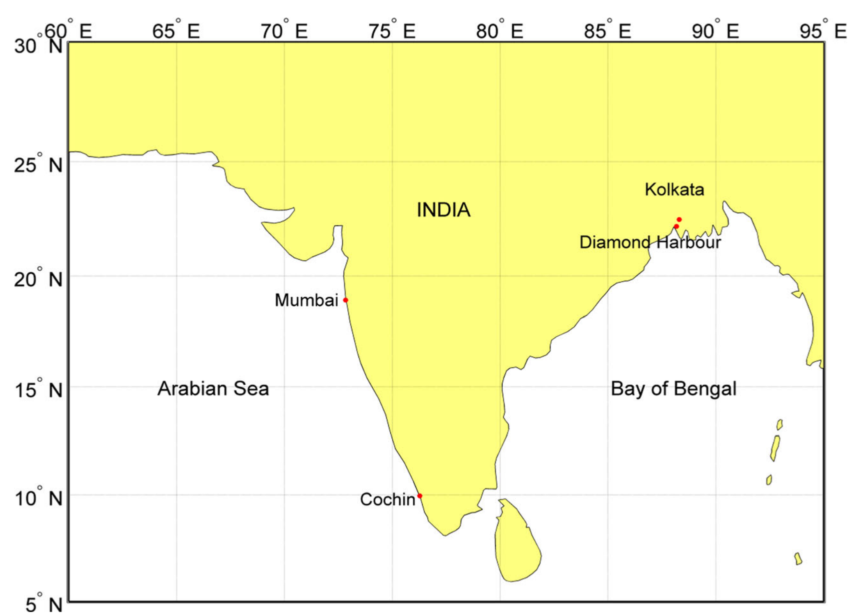

Fig. 1 Approximate geographical location of different tide gauges along the coast of India

Table 2 Location details of different tide gauge locations with permanent service for mean sea level (PSMSL) ID

Tide gauge name	PSMSL ID	Latitude (degrees)	Longitude (degrees)
Diamond Harbour	543	22.2	88.17
Kolkata	369	22.55	88.3
Cochin	32	9.96	76.27
Mumbai	43	18.91	72.83

gauging sites. It is felt necessary to check the data homogeneity at Kolkata before proceeding to statistical analyses and model development. The statistical tests for checking the homogeneity of variance are based on the null hypothesis that the data is homoscedastic, i.e. homogeneity of variance against the alternative hypothesis that it is not. The tests were done at 5 % significance level. The details of the test results are as follows:

1. The homogeneity of variance of observed sea level between Diamond Harbour and Kolkata is checked by using Welch test. In Welch test, the monthly observed sea level record during the historical period of Kolkata and Diamond Harbour is considered as two different samples. The assumption of homoscedasticity between the data of Kolkata and Diamond Harbour was acceptable at 5 % significance level.
2. The homogeneity of variance of the observed sea level during historical period of Kolkata used for model development is checked by the following five different statistical tests:

   (i) Bartlett test
   (ii) Cochran test
   (iii) Levenes test
   (iv) Brown-Forsythe test
   (v) O'Brien test

The data of Kolkata tide gauge during historical period is divided into five different samples for carrying out the aforementioned statistical tests. The assumption of homoscedasticity was met using all the five tests at 5 % significance level.

3. The homogeneity of mean of observed sea level time series during historical period at Kolkata is checked by using the Pettit's test at 5 % significance level. The assumption of homogeneity of mean was acceptable using Pettit's test.

Next, the model development and its validation are carried out for each of the tide gauge individually. The model parameters, as discussed in methodology, are the constant term 'c' and the slope obtained by the fit between the CI anomaly and the observed sea level rate anomaly. Since the anomaly value is used, the constant term 'c' is almost equal to zero. The computed SPCA coefficients obtained in the development period are used for developing the CI in the testing and the projection period. The square of the SPCA coefficients corresponding to a particular climate variable represents the relative weightage of that climate variable to cause the SLC with respect to set of other climate variables considered. It may be noted that the sum of square of SPCA coefficients of all the inputs (ATP, UWN, VWN, SLP, PPT) at a particular tide gauge is unity. Thus, the climate variable for which the absolute value of SPCA coefficient is minimum is deemed to have the lowest effect on the local SLC.

Estimated model parameters at the different tide gauges are shown in Table 4. The good performance of the model with high CC and DoA is achieved for all the tide gauges. This is true for both model development and testing periods. The good performance statistics indicate that the linear variation of considered climate inputs with respect to SLC is reasonably acceptable if not excellent, given the complexity involved in the problem at hand. Diamond harbour located in the northern interior of Bay of Bengal has a continuously rising sea level during the period 1948–1996. It can be noted from the coefficients of the CI obtained through SPCA at Diamond harbour

Table 3 Period of analysis at different tide gauges

Tide gauge	Development period	Testing period	Future projection period
Diamond Harbour	1948–1996	1999–2005	2006–2100
Kolkata	1948–1990	1991–1996	2006–2100
Cochin	1948–1996	1997–2005	2006–2100
Mumbai	1948–1985	1986–1994	2006–2100

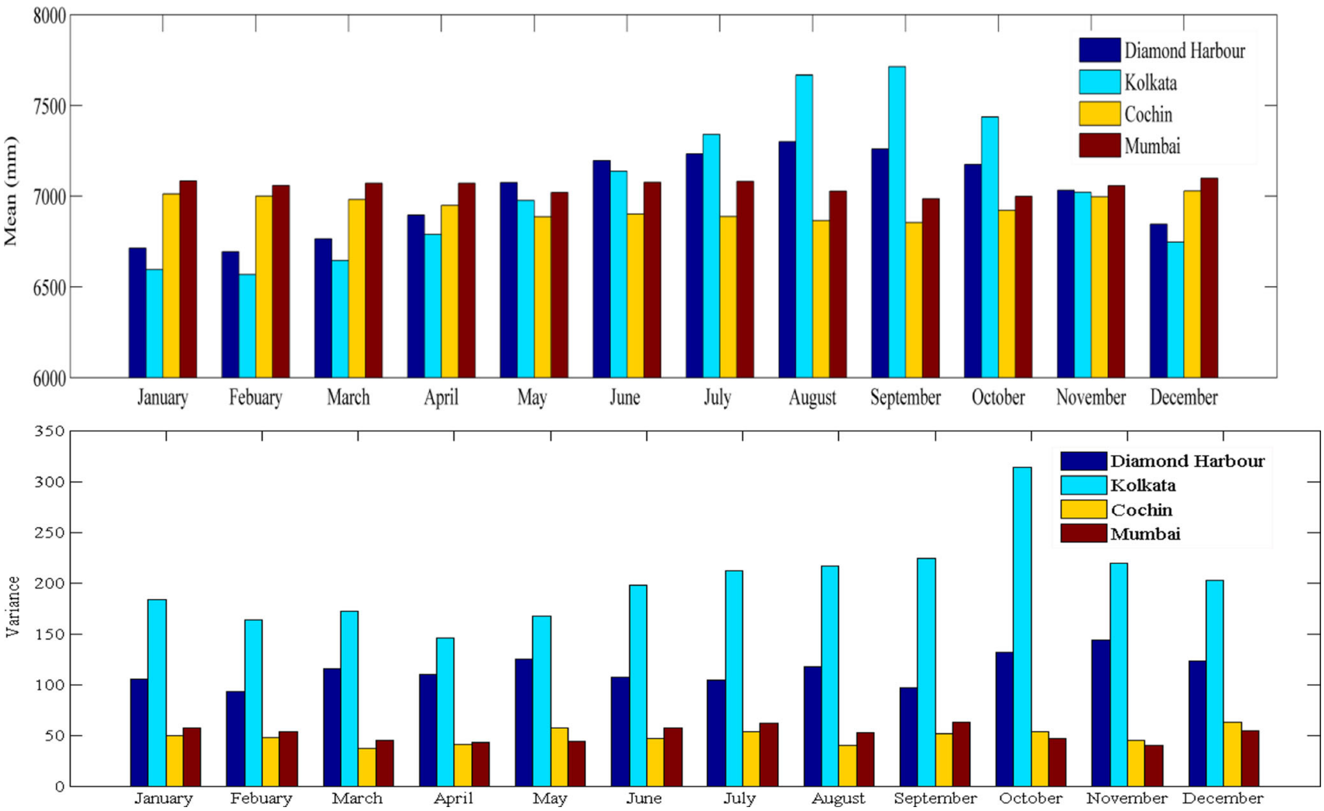

Fig. 2 Long term monthly mean and standard deviation during the model development period for different tide gauges under study

that the ATP (0.009) has the lowest weightage in comparison to the other variables behind SLC at Diamond Harbour and the highest weightage is from the SLP (0.64). The VWN (−0.618) also plays a significant part in simulating SLC at Diamond Harbour. These coefficients thus signify the underlying relative importance of climate variables with respect to SLC. The model performance at Diamond Harbour is good both during the model development and model testing period. The model performance statistics during the development and the testing periods are shown in Table 5.

The performance of the model at Kolkata is good with high CC and DoA. The coefficients of hydroclimatic inputs while developing CI for ATP, UWN, VWN, SLP and PPT are −0.259, −0.368, −0.429, 0.704 and 0.340, respectively, that imply the highest influence is due to SLP (0.704). The ATP (−0.259) has a more significant role behind the SLC at Kolkata as compared to Diamond Harbour. The coefficients UWN, VWN, PPT and SLP obtained at Kolkata are almost similar to that obtained at Diamond Harbour.

Cochin located along the western coast of Indian subcontinent has a different climate anomaly when compared to the two eastern coast tide gauges discussed before. The coefficients of CI obtained for ATP, UWN, VWN, SLP and PPT are −0.147, −0.457, 0.329, −0.515 and 0.629, respectively. Although the coefficient of SLP (−0.515) is pronounced, the influence of UWN (−0.457) and PPT (0.629) on SLC at Cochin is more prominent. The performance of the proposed method at Cochin in the development and testing period (CC = 0.79 and DoA = 0.70 during the model development period and CC = 0.76 and DoA = 0.67 during the model testing period) is a little poorer as compared to Diamond Harbour and Kolkata. The reason for decrease in performance at Cochin could be because of higher number of missing observed tidal gauge data (monthly) from the PSMSL. A total of 41 monthly values during the development period and 20 monthly values during the testing period at Cochin are missing.

The Mumbai tide gauge is also situated along the western coast on the Arabian Sea towards the north of Cochin. It is one of the oldest tidal gauge locations of India which is having the record from the year 1878. The coefficients of hydroclimatic inputs while developing CI are 0.389, −0.456, 0.478, −0.583 and 0.269 for ATP, UWN, VWN, SLP and PPT, respectively, showing the wind and pressure components having higher effect on SLC at Mumbai. The model performance at Mumbai in the development period (CC = 0.62 and DoA = 0.61) and the testing period (CC = 0.69 and DoA = 0.66) is not as high as Diamond Harbour and Kolkata. The reason of a little poorer performance of the model at Mumbai could not be definitely deduced. However, since the record of observed sea level from PSMSL for Mumbai is much longer, the analysis at Mumbai was repeated for a

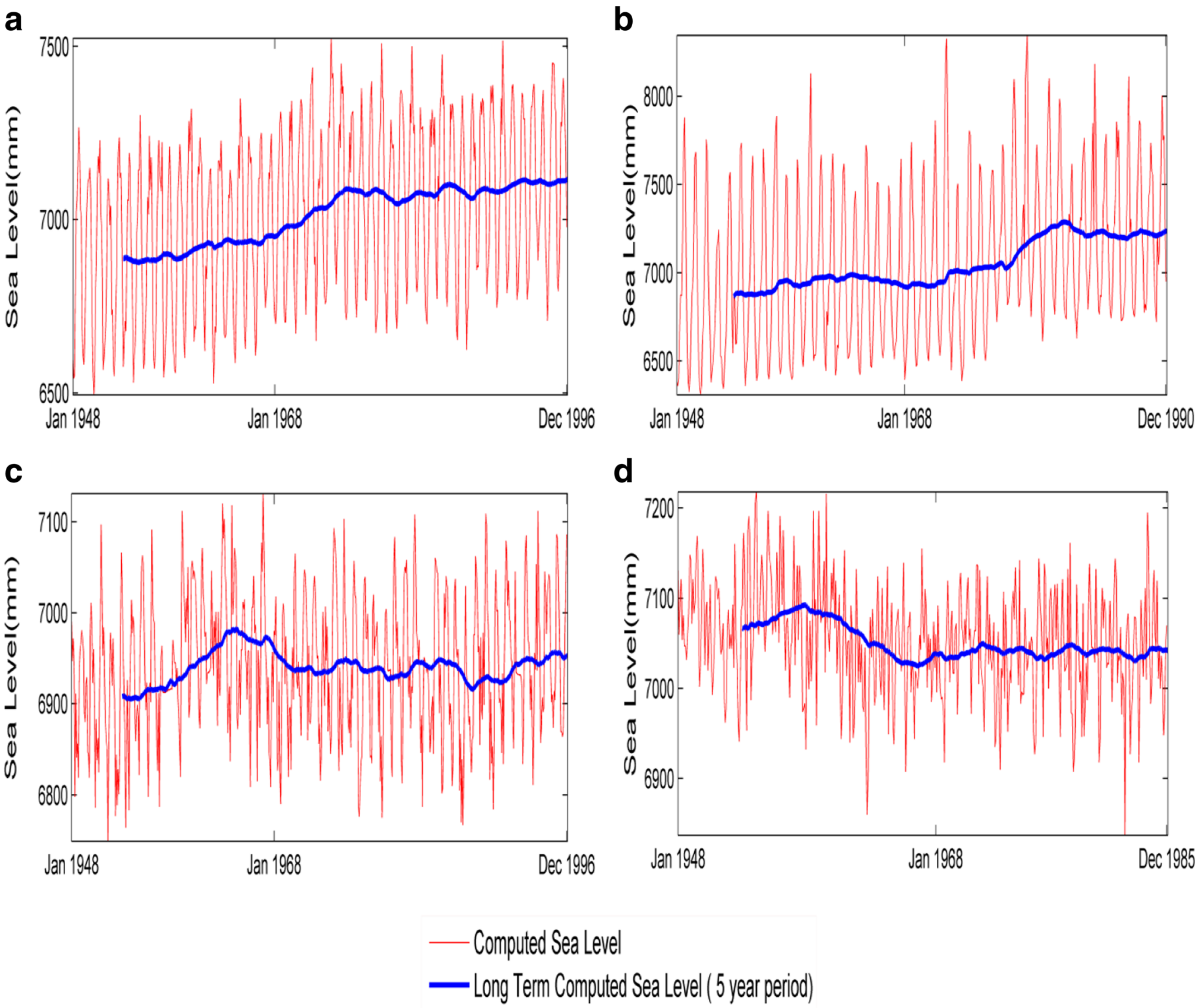

Fig. 3 Plot of observed sea level at **a** Diamond Harbour, **b** Kolkata, **c** Cochin and **d** Mumbai

separate set of model development (1880–1930) and model testing periods (1931–1950). The obtained CC and DoA values are 0.55 and 0.62, respectively, during the development period. During the testing period, these values are 0.56 and 0.62, respectively. This signifies that change in the model development and testing period at Mumbai has not affected the final model performance. The comparison plots between the estimated and the observed sea level in the model development and testing period at the four coastal locations under study are shown in Figs. 5 and 6, respectively. It can be noted from Fig. 5 that sea level observed in Arabian Sea (both Cochin and Mumbai) is almost straight specifically after the year 1960 until 1990. However, there is a rise in sea level at Cochin and Mumbai after the year 1990 (refer Figs. 6 and 7). It is perhaps due to the fact that the effect of climate change induced local SLR in Arabian sea is realized more recently (post 1990s). We like to reiterate in this context that the proposed approach is able to successfully model the sea level rise at local scale considering the combined effect of hydro-climatic variables. Before 1990, when the sea levels were almost straight, and after 1990s, when the sea levels rise is realized, the proposed model successfully captures both the scenarios. Thus, the developed Combined Index (CI) is potential in capturing the local SLR. We like to further emphasize the point that an individual hydro-climate variable may not always truly model the rise at local scale. The concurrent effect of all the potential hydro-climatic variables is important to consider. It is further noticed from the computed sea level (Fig. 5) that the magnitude of SLC obtained at Diamond Harbour and Kolkata during the development period is higher when compared with the SLC magnitude obtained at Cochin and Mumbai. This signifies that the SLR at these two tide gauges located on the eastern coast of India is higher than those on the western coast during the historical period.

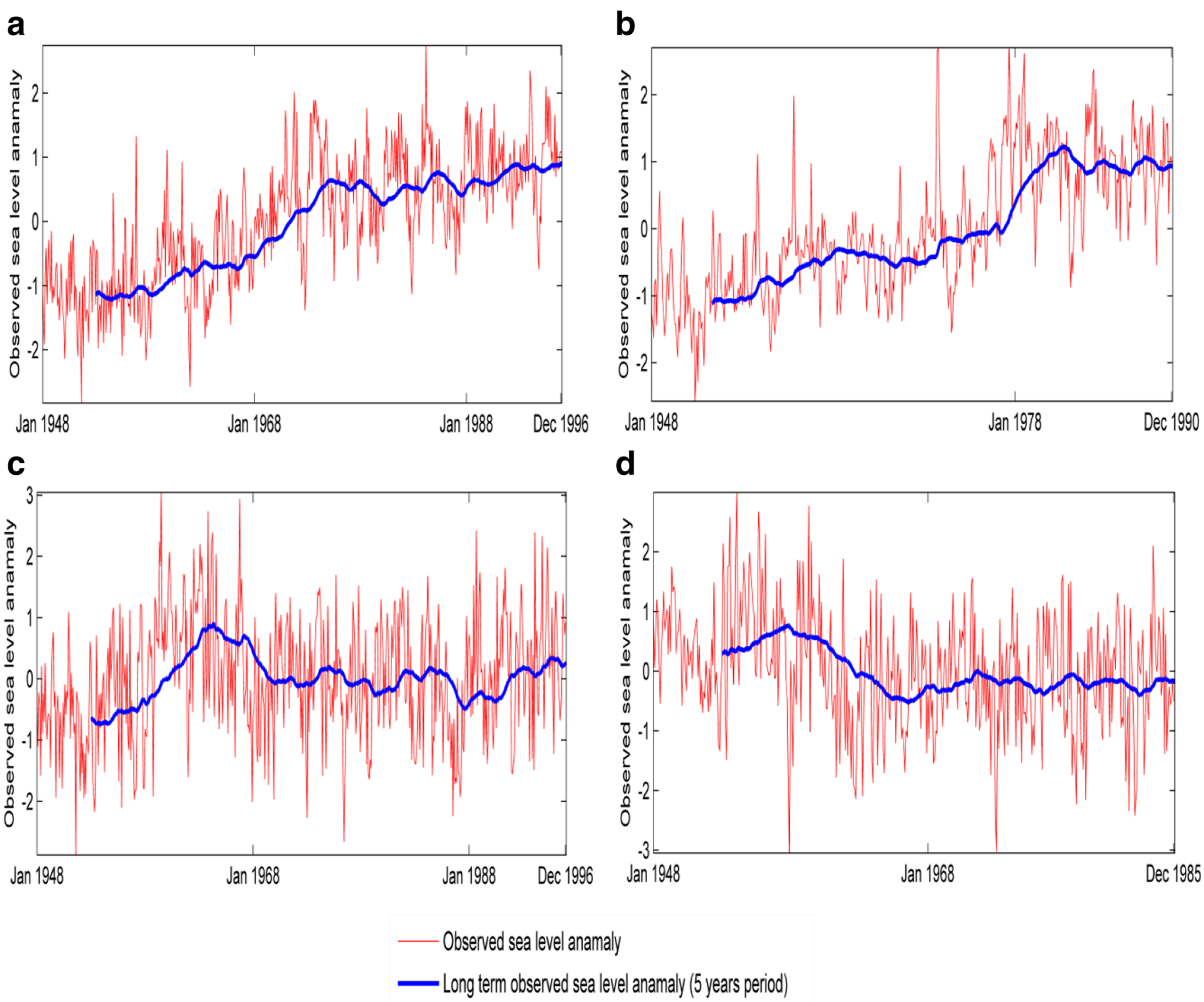

Fig. 4 Plot of observed sea level anomaly at **a** Diamond Harbour, **b** Kolkata, **c** Cochin and **d** Mumbai

4 Future projection of local sea level rise

In this section, separate projections of local SLR for three different future scenarios of RCPs (RCP2.6, RCP4.5, RCP8.5) are carried out at different tide gauges, mentioned before. Before that, a small discussion on rise in GMSL is presented since this is used in the final LSL computation. The SLR in the twenty-first century will be more due to the climatic factors, e.g. rising temperature and its consequence, such as ice sheet melting. The effect of other factors like land water storage, anthropogenic causes would be less for the rise in this century (Church and Clark, 2013). RCP6.0 is not considered since its global sea level projections are similar to that of RCP4.5. GMSL in the year 2081–2100 will likely be in the

Table 4 Model parameter and coefficients of different inputs as obtained from SPCA during model development period. For abbreviations, please refer to the text

Tide gauge	Model parameter (θ)	Coefficients of different inputs				
		ATP	UWN	VWN	SLP	PPT
Diamond Harbour	0.28	0.009	−0.262	−0.618	0.640	0.372
Kolkata	0.32	−0.259	−0.368	−0.429	0.704	0.340
Cochin	0.31	−0.147	−0.457	0.329	−0.515	0.629
Mumbai	0.32	0.389	−0.456	0.478	−0.583	0.269

Table 5 Model performance statistics during model development and testing periods at different tide gauges

Tide gauge	Model development period			Model testing period		
	CC	RMSE (mm)	DoA	CC	RMSE (mm)	DoA
Diamond Harbour	0.89	141.19	0.79	0.93	103.72	0.84
Cochin	0.79	15.4553	0.70	0.76	74.99	0.67
Kolkata	0.90	255.40	0.79	0.95	2.19	0.86
Mumbai	0.62	21.87	0.61	0.69	37.11	0.66

ranges of 0.26 to 0.55 m for RCP2.6, 0.32 to 0.63 m for RCP4.5, 0.33 to 0.63 m for RCP6.0 and 0.45 to 0.82 for RCP8.5. The rate of SLR is estimated to be 8 to 16 mm per year for RCP8.5 during 2081 to 2100. The projected climate for the next few decades will be having spatial patterns of change with lesser magnitude when compared with the later decades in twenty-first century. The definite range of changes of hydroclimatic variables for a particular RCP over the period

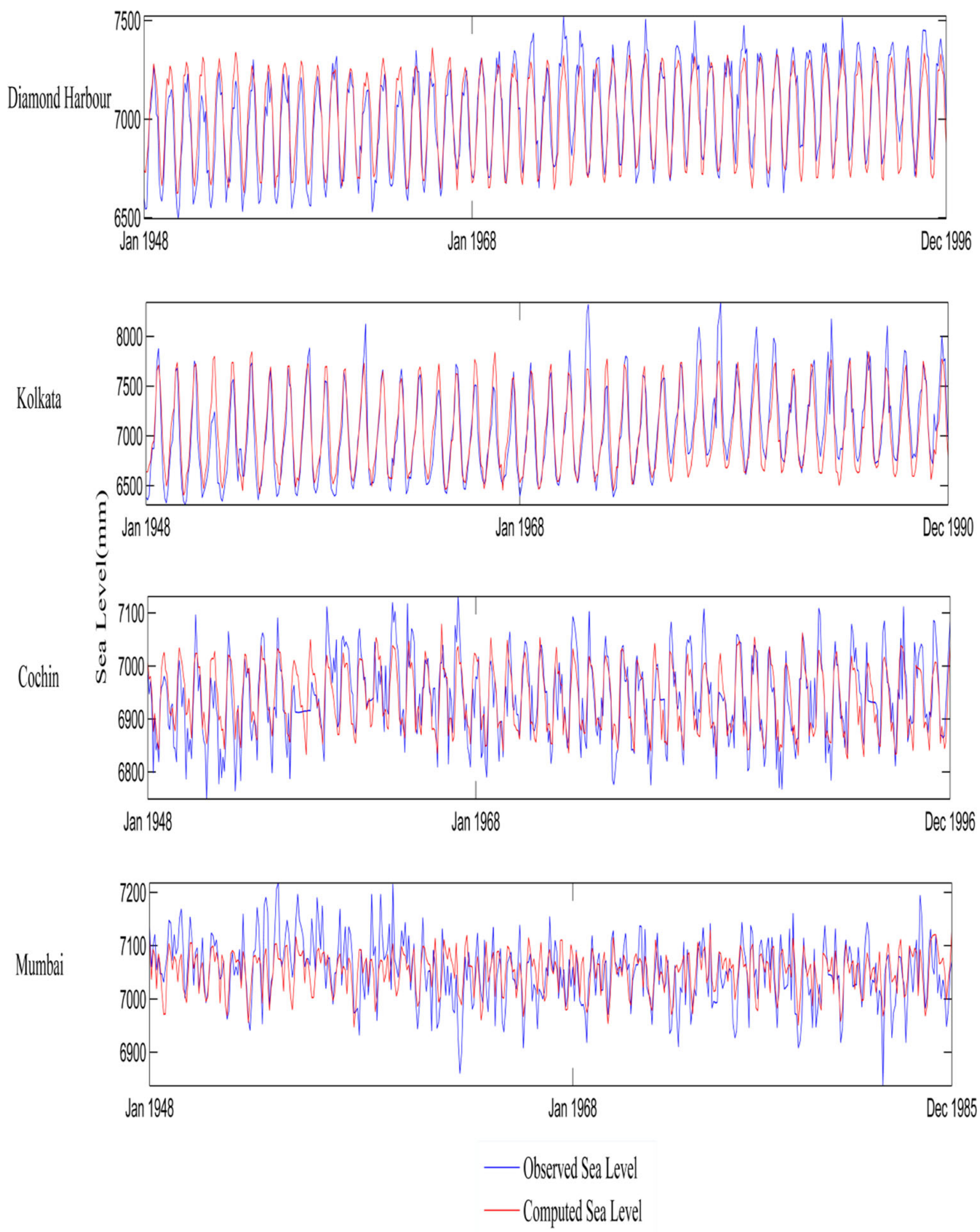

Fig. 5 Plot between computed and observed sea level during model development period at different tidal gauge locations

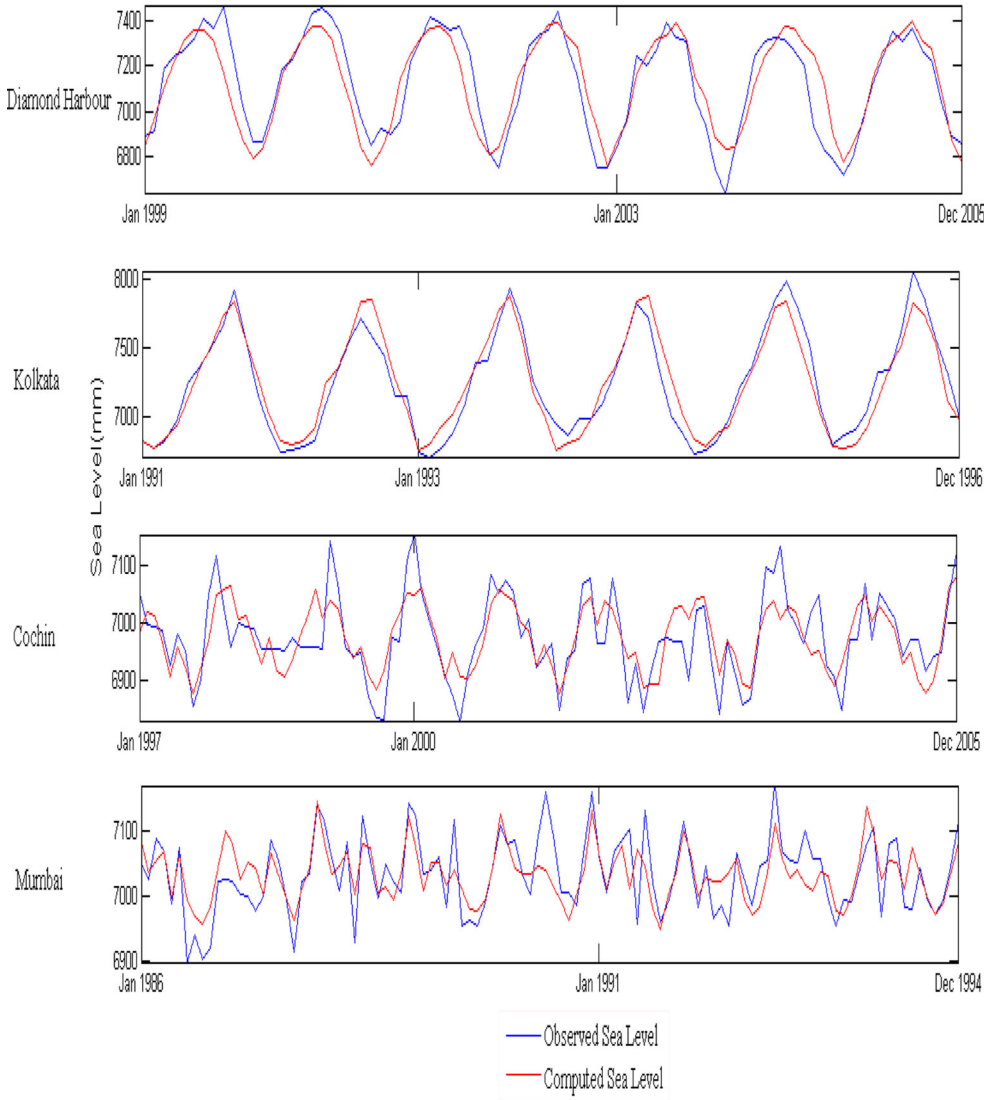

Fig. 6 Plot between computed and observed sea level during model testing period at different tidal gauge locations

in the twenty-first century can be seen comprehensively from the IPCC AR5. In this section, the climate induced SLR projection analysis is carried out using the developed model.

The monthly SLR in the twenty-first century at the four tide gauges is projected using the proposed model with the calibrated model parameters. The climate projections of CanESM2 are used to develop the CI during the projection period. The SLR at the end of year 2100 is computed in terms of rise above the sea level in a particular benchmark year. Thus, the projected SLR indicates a relative rise with respect to the benchmark year. The benchmark year is considered as the year 1984 for all the four tide gauges.

The projected SLR at different tide gauges is shown in Fig. 7. At a particular station, three different projections are presented for three different future scenarios. For instance, the projected rise at Diamond Harbour by the year 2100 is 105.38 mm in case of RCP2.6. This value is found to increase to 163.67 and 287.92 mm in case of RCP4.5 and RCP8.5, respectively. At Cochin, rise of 123.92 mm is projected by the end of the year 2100 according RCP2.6. Similarly, a rise of 171.10 and 305.85 mm is noticed in case of RCP4.5 and RCP8.5, respectively. The rise at Mumbai is computed to be 120.48, 178.71 and 308.18 mm in case of RCP2.6, RCP4.5 and RCP8.5, respectively. The projection of sea level at Kolkata is noticed to be minimum as compared to other tide gauges. The value of SLR is 55.05, 121.92 and 239.85 mm is expected by the end of twenty-first century in case of RCP2.6, RCP4.5 and RCP8.5, respectively. It may be noted here that the climate forcing in case of RCP8.5 scenario is highest among all other RCPs. It is found in this analysis that the projected SLR in case of RCP8.5 is highest among all other future climate change scenarios. This is true for all the four tide gauges though the individual values are different from each other.

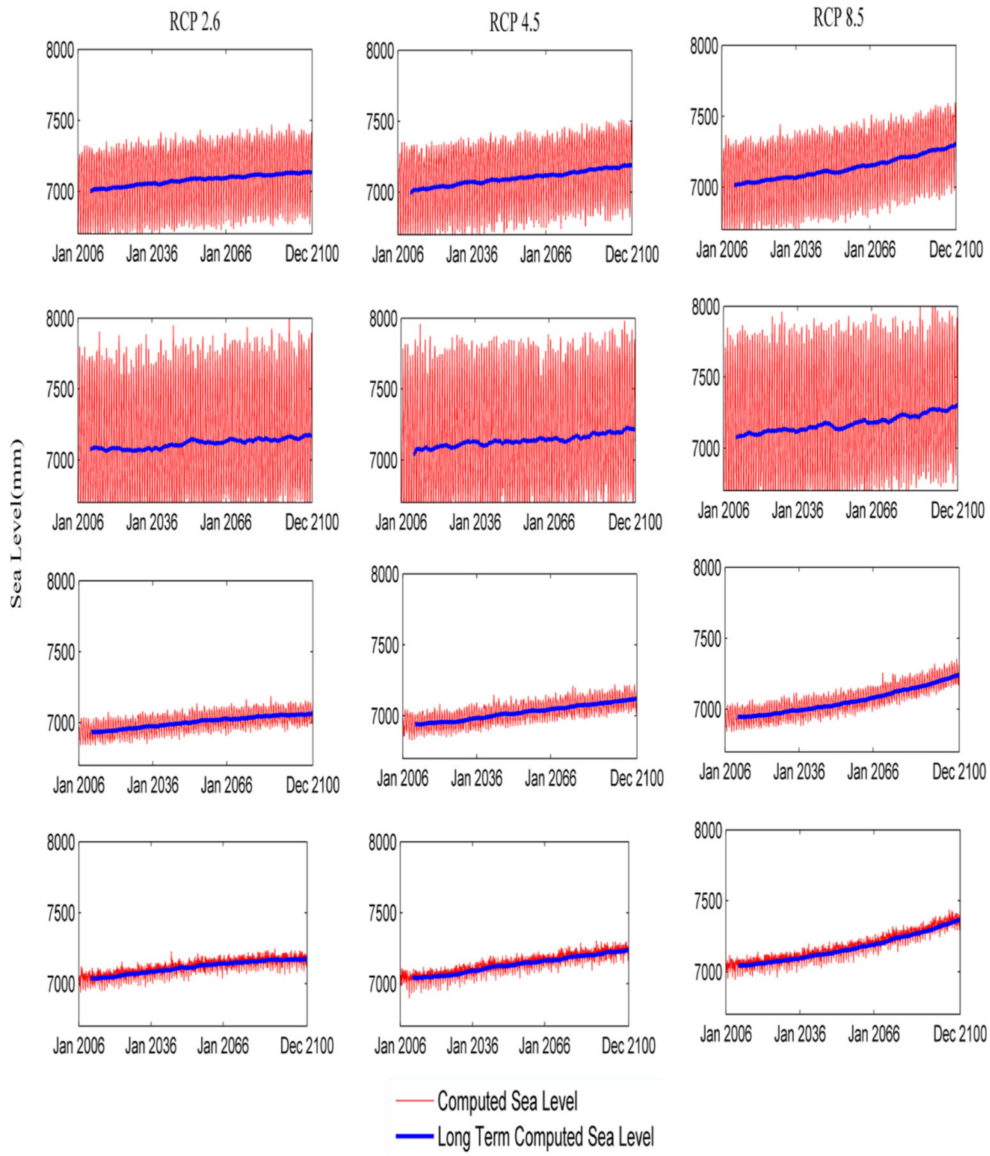

Fig. 7 Plot of projected local sea level variation during twenty-first century at Diamond Harbour (*1st row*), Kolkata (*2nd row*), Cochin (*3rd row*) and Mumbai (*last row*) for RCP2.6 (*left column*), RCP4.5 (*middle column*) and RCP6.0 (*right column*)

It is noticed before that the tide gauges along the eastern coast (i.e. Diamond Harbour and Kolkata) experience higher magnitude of SLC as compared to the tide gauges along the western coast (i.e. Cochin and Mumbai) during the historical period. However, the SLR projections observed at Mumbai and Cochin by the year 2100 are higher as compared to the same at Diamond Harbour and Kolkata. This signifies that even though a coastal location may experience lesser magnitude of SLC or no pronounced rise in the past, the same behaviour of SLC or rise may not be expected during the future. Another point is that the methodology proposed in this study is general in nature and can be applied to any other location in the world. However, being a data-driven approach, sufficient length of data is required to develop the CI for a new location. Investigation on the spatial transferability of the proposed approach would be a potential future scope of this study that will help to project SLR at an ungauged location.

5 Conclusions

In this paper, a methodological approach is proposed to model local SLR. The developed approach utilizes different hydroclimatic variables as input that is proven to have their influence on SLC. The approach is particularly important in the context of climate change since the change in climatic factors, if any, is being considered through a combined index. Air temperature, zonal wind, meridional wind, sea level pressure and precipitation constitute the set of input variables. The developed approach is applied to four different locations along Indian coast—two along the Bay of Bengal and two along the Arabian Sea.

The developed semi-empirical model is simpler in its form and has the flexibility to incorporate as many number of climate inputs which are suspected to cause the SLC. The potential use of SPCA in blending the different hydroclimatic inputs with proper weightages (coefficients) to develop a combined index for modelling the SLCs is demonstrated. The relative importance of each of the climate input in estimating the SLC can also be assessed through the coefficients obtained through SPCA. It is noticed that the relative importance of each input variable varies from one location to another, causing perhaps one of the reasons behind spatial variation in local SLR. The performance of the model is found to be reasonably good during both model development and testing period at all the tide gauges with best performance statistics at Diamond Harbour and lowest performance statistics at Mumbai over the historical period.

Future projection of local SLR for three different scenarios (RCP2.6, RCP4.5 and RCP 8.5) reveals a warning situation for all the locations considered in this study. In particular, the SLR at Mumbai (308.18 mm) and Cochin (305.85 mm) by the year 2100 is slightly higher than that at Diamond Harbour (287.92 mm) and Kolkata (239.85 mm) by the year 2100 for the worst future scenario (i.e. RCP8.5). This study further indicates that the observed rate of SLR in the historical data does not necessarily continue at the same rate in the future.

The proposed methodology is general in nature and can be applied for any coastal location worldwide depending upon the availability of observed tidal gauge records and hydroclimatic variables. However, a sufficiently long data record is necessary to estimate the model parameters and combined index. Spatial transferability of the proposed approach is kept as the future scope of this study.

Acknowledgments This work is supported by the Ministry of Human Resources Development (MHRD) through a sponsored project 'Future of Cities (FoC)' (F. NO. 4-22/2014-TS.I, Dt. 23-01-2014).

References

Albrecht F, Weisse R (2012) Pressure effects on past regional sea level trends and variability in the German Bight. Journal of Ocean Dynamics 62:1169–1186. doi:10.1007/s10236-012-0557-1

Barshan E, Ghodsi A, Azimifar Z, Jahromi MZ (2011) Supervised principal component analysis: visualization, classification and regression on subspaces and submanifold. Pattern Recogn 44: 1357–1371. doi:10.1016/j.patcog.2010.12.2015

Bindoff NL, Willebrand J, Artale V, Cazenave A, Gregory J, Gulev S, Hanawa K, Le Quéré C, Levitus S, Nojiri Y, Shum CK, Talley LD, Unnikrishnan A (2007) Observations: oceanic climate change and sea level. In: Solomon S, Qin D, Manning M, Chen Z, Marquis M, Averyt KB, Tignor M, Miller HL (eds) In: climate change 2007: the physical science basis, contribution of working group I to the fourth assessment report of the intergovernmental panel on climate change. Cambridge University Press, Cambridge, United Kingdom and New York, NY, USA

Church JA, Clark U (2013) IPCC fifth assessment report: Sea level change (Chapter 13). pp 1137–1215 Available at www.ipcc.ch

Dogan M, Cigizoglu HK, Sanli DU, Ulke A (2015) Investigation of sea level anomalies related with NAO along the west coasts of Turkey and their consistency with sea surface temperature trends. Theor Appl Climatol 121(1):349–358. doi:10.1007/s00704-014-1247-3

Frankignoul C, Müller P, Zorita E (1997) A simple model of the decadal response of the ocean to stochastic wind forcing. J Phys Oceanogr 27:1533–1546. doi:10.1175/1520-0485(1997)0272.0.co;2

Grinsted A, Moore JC, Jevrejeva S (2010) Reconstructing sea level from paleo and projected temperatures 200 to 2100AD. Clim Dyn 34: 461–472. doi:10.1007/s00382-008-0507-2

Han G, Huang W (2009) Low-frequency sea-level variability in the South China Sea and its relationship with ENSO. Theor Appl Climatol 97(1):41–52. doi:10.1007/s00704-008-0070-0

Hong BG, Sturges W, Clarke AJ (2000) Sea level on the U.S. east coast: decadal variability caused by open ocean wind-curl forcing. Journal of Physical Oceanography 30:2088–2098, doi:10.1175/1520–0485(2000) 0302.0.co;2

Horton RM, Gornitz V, Bader DA, Ruane AC, Goldberg R, Rosenzweig C (2011) Climate hazard assessment for stakeholder adaptation planning in New York City. J Appl Meteorol Climatol 50:2247–2266. doi:10.1175/2011jamc2521.1

Hunicke B, Zorita E (2006) Influence of temperature and precipitation on decadal Baltic Sea level variations in the 20th century. Tellus A 58: 141–153. doi:10.1111/j.1600-0870.2006.00157.x

Jevrejeva S, Grinsted A, Moore JC (2009) Anthropogenic forcing dominates sea level rise since 1850. Geophys Res Lett 36:L20706. doi:10.1029/2009gl040216

Jevrejeva S, Moore JC, Grinsted A (2010) How will sea level respond to changes in natural and anthropogenic forcing by 2100? Geophys Res Lett 37:L07703. doi:10.1029/2010gl042947

Katsman C, Sterl A, Beersma J, van den Brink H, Church J, Hazeleger W, Kopp R, Kroon D, Kwadijk J, Lammersen R, Lowe J, Oppenheimer M, Plag H, Ridley J, Von Storch H, Vaughan D, Vellinga P, Vermeersen L, van de Wal R, Weisse R (2011) Exploring high-end scenarios for local sea level rise to develop flood protection strategies for a low-lying delta the Netherlands as an example. Clim Chang 109:617–645. doi:10.1007/s10584-011-0037-5

Kemp AC, Horton BP, Donnelly JP, Mann ME, Vermeer M, Rahmstorf S (2011) Climate related sea-level variations over the past two millennia. Proceedings of National Academy of Sciences 108: 11017–11022. doi:10.1073/pnas.1015619108

Kolker AS, Hameed S (2007) Meteorologically driven trends in sea level rise. Geophys Res Lett 34:L23616. doi:10.1029/2007gl031814

Kopp RE, Horton RM, Little CM, Mitrovica JX, Oppenheimer M, Rasmussen DJ, Strauss BH, Tebaldi C (2014) Probabilistic 21st and 22nd century sea-level projections at a global network of tide-gauge sites. Earth's Future 2:383–406. doi:10.1002/2014ef000239

Kopp RE, Mitrovica JX, Griffies SM, Yin J, Hay CC, Stouffer RJ (2010) The impact of Greenland melt on local sea levels: a partially coupled analysis of dynamic and static equilibrium effects in idealized water-hosing experiments. Climate Change 103:619–625. doi:10.1007/s10584-010-9935-1

Levermann A, Clark PU, Marzeion B, Milne GA, Pollard D, Radic V, Robinson A (2013) The multimillennial sea-level commitment of global warming. Proceedings of National Academy of Sciences 110:13745–13750. doi:10.1073/pnas.1219414110

Lowe J, Gregory J (2006) Understanding projections of sea level rise in a Hadley Centre coupled climate model. J Geophys Res 111:C11014. doi:10.1029/2005jc003421

Meehl GA, Covey C, Delworth T, Latif M, McAvaney B, Mitchell JFB, Stouffer RJ, Taylor KE (2007a) The WCRP CMIP3 multi-model dataset: a new era in climate change research. Bulletin of American Meteorological Society 88:1383–1394. doi:10.1175/bams-88-9-1383

Meehl GA, Stocker TF, Collins WD, Friedlingstein P, Gaye AT, Gregory JM, Kitoh A, Knutti R, Murphy JM, Noda A, Raper SCB, Watterson IG, Weaver AJ, Zhao ZC (2007b) Global climate projections. In: Solomon S, Qin D, Manning M, Chen Z, Marquis M, Averyt KB, Tignor M, Miller HL (eds) In: climate change 2007: the physical science basis. Contribution of working group I to the fourth assessment report of the intergovernmental panel on climate change. Cambridge University Press, Cambridge, United Kingdom and New York, NY, USA

Miller KG, Kopp RE, Horton BP, Browning JV, Kemp AC (2013) A geological perspective on sea-level rise and impacts along the U.S. mid-Atlantic coast. Earth's Future 1:3–18. doi:10.1002/2013ef000135

Milne GA, Gehrels WR, Hughes CW, Tamisiea ME (2009) Identifying the causes of sea-level change. Natural Geoscience 2:471–478. doi:10.1038/ngeo544

NYCPCC, edited by Rosenzweig C, Solecki W, NPCC2 (2013) Climate risk information: observations, climate change projections and maps. Prepared for use by the City of New York Special Initiative on Rebuilding and Resiliency, New York

Pardaens AK, Lowe JA, Brown S, Nicholls RJ, de Gusmão D (2011) Sea-level rise and impacts projections under a future scenario with large greenhouse gas emission reductions. Geophys Res Lett 38:L12604. doi:10.1029/2011gl047678

Perrette M, Landerer F, Riva R, Frieler K, Meinshausen M (2013) A scaling approach to project regional sea level rise and its uncertainties. Earth System Dynamics 4:11–29. doi:10.5194/esd-4-11-2013

Rahmstorf S (2007) A semi empirical approach to projecting future sea-level rise. Science 315:368–370. doi:10.1126/science.1135456

Slangen AB, Carson M, Katsman CA, van de Wal RSW, Köhl A, Vermeersen LLA, Stammer D (2014) Projecting twenty-first century regional sea level changes. Climate Change 124:317–332. doi:10.1007/s10584-014-1080-9

Slangen ABA, Katsman CA, van de Wal RSW, Vermeersen LLA, Riva REM (2012) Towards regional projections of twenty-first century sea-level change based on IPCC SRES scenarios. Clim Dyn 38:1191–1209. doi:10.1007/s00382-011-1057-6

Solomon S, Plattner G, Knutti R, Friedlingstein P (2009) Irreversible climate change due to carbon dioxide emissions. Proceedings of National Academy of Sciences 106:1704–1709. doi:10.1073/pnas.0812721106

Stammer D, Cazenave A, Ponte RM, Tamisiea ME (2013) Causes for contemporary regional sea level changes. Annual Review of Marine Science 5:21–46. doi:10.1146/annurev-marine-121211-172406

Suzuki T, Ishii M (2011) Long-term regional sea level changes due to variations in water mass density during the period 1981–2007. Geophys Res Lett 38:L21604. doi:10.1029/2011gl049326

Timmermann A, McGregor S, Jin FF (2010) Wind effects on past and future regional sea level trends in the Southern Indo-Pacific. J Clim 23:4429–4437. doi:10.1175/2010jcli3519.1

Vermeer M, Rahmstorf S (2009) Global sea level linked to global temperature. Proceedings of National Academy of Sciences 106:21527–21532. doi:10.1073/pnas.0907765106

Willmott CJ, Robesonb SM, Matsuuraa K (2012) A refined index of model performance. Int J Climatol 32:2088–2094. doi:10.1002/joc.2419

Wunsch C, Stammer D (1997) Atmospheric loading and oceanic inverted barometric effect. Rev Geophys 35:79–107. doi:10.1029/96rg03037

Yin J, Schlesinger ME, Stouffer RJ (2009) Model projections of rapid sea-level rise on the northeast coast of the United States. Nat Geosci 2:262–266. doi:10.1038/ngeo462